

GRAIN ALIGNMENT BY RADIATION IN DARK CLOUDS AND CORES

JUNGYEON CHO

Dept. of Astronomy and Space Science, Chungnam National University, Daejeon, Korea; jcho@cnu.ac.kr

AND

A. LAZARIAN

Astronomy Dept., Univ. of Wisconsin, Madison, WI53706, USA; lazarian@astro.wisc.edu

Draft version January 3, 2019

ABSTRACT

We study alignment of grains by radiative torques. We found steep rise of radiative torque efficiency as grain size increases. This allows larger grains that are known to exist within molecular clouds to be aligned by the attenuated and reddened interstellar radiation field. In particular, we found that, even deep inside giant molecular clouds, e.g. at optical depths corresponding to $A_V \lesssim 10$, large grains can still be aligned by radiative torque. This means that, contrary to earlier claims, far-infrared/submillimeter polarimetry provides a reliable tool to study magnetic fields of pre-stellar cores. Our results show that the grain size distribution is important for determining the relation between the degree of polarization and intensity.

Subject headings: ISM: dust, extinction — ISM: clouds — polarization — radiative transfer

1. INTRODUCTION

It is widely believed that magnetic fields play a crucial role for the dynamics of molecular clouds and for the star formation processes (see review by Crutcher 2004 and references therein).¹ One of the most informative techniques of studying magnetic fields in molecular clouds is based on the use of starlight polarization and polarized emission arising from aligned dust.

Alignment of interstellar dust was not expected by theorists. Very soon after the discovery of the interstellar origin of starlight polarization by Hall (1949) and Hiltner (1949), it became clear that interstellar grains get aligned with respect to magnetic field. It did not take long time to realize that grains tend to be aligned with their long axes perpendicular to magnetic field. However, progress in theoretical understanding of the alignment has been surprisingly slow in spite of the fact that great minds like L. Spitzer and E. Purcell worked on grain alignment (see Spitzer & Tukey 1951, Purcell 1969, Spitzer & Purcell 1971, Purcell 1975, 1979, Spitzer & McGlynn 1979). The problem happened to be very tough and a lot of relevant physics had to be uncovered. An extended discussion of different proposed mechanisms with the relevant references can be found in a recent review by Lazarian (2003).

Originally it was widely believed that interstellar grains can be well aligned by a paramagnetic mechanism (Davis & Greenstein 1951). This mechanism, based on the direct interaction of rotating grains with the interstellar magnetic field, required magnetic fields that are substantially stronger than those uncovered by other techniques.² Later, a pioneering work by Purcell (1979, henceforth P79) showed a way how to make grain alignment more efficient. Purcell noticed that grains rotating at high rates are less susceptible to the randomization induced by gaseous collisions, while paramagnetic alignment would proceed at the same rate. He introduced several processes that are bound to make grains very fast “suprathermal” rotators. They are a) variations of the accommodation coefficient for atoms and molecules bouncing from the grain surface, b) variations of the coefficient of electron ejection, c) variations of the sites of H₂ formation over grain surface. As H₂ formation over grain surfaces is a common interstellar process and every formation event could deposit an appreciable angular momentum with the grain, Purcell identified c) as the major cause of grain fast rotation. He claimed that the catalytic sites ejecting H₂ molecules (frequently called “Purcell’s rockets”) should spin up grains very efficiently for most of the diffuse ISM. One can easily see that within the Purcell’s model, even a small fraction of atomic hydrogen present in molecular clouds would also make them suprathermal (i.e. $E_{kin} \gg kT_{grain}$). For decades this became a standard explanation for grain alignment puzzle, although it could not explain several observational facts, e.g. why observations indicate that small grains are less aligned than the large ones.

New physics of grain internal motion uncovered fairly recently explains why small grains are poorly aligned by Purcell’s mechanism. The inefficiency stems from grain internal wobbling. Indeed, for sufficiently small grains it is impossible to assume that they rotate perfectly about their axis of maximal inertia. It is interesting to recall that the issue of grain wobbling was a part of the alignment process discussed e.g. by Spitzer (see Jones & Spitzer 1968).

¹ Existing claims of the contrary (see Padoan & Norlund 1998) make quantitative studies of magnetic fields more essential.

² As discussed, for instance in Lazarian (2003), the very small grains are likely to be aligned by this mechanism and this can explain the peculiarities of the UV part of the spectrum of the polarized radiation observed (see Kim & Martin 1995). The alignment of small grains by paramagnetic relaxation is possible as efficiency of the Davis-Greenstein mechanism increases as the grain size decreases. The degree of alignment of small grains provides a direct constrain on the intensity of magnetic field, which is a subject that calls for more of UV polarimetry work.

However, when P79 identified Barnett relaxation as an fast process of internal relaxation that aligns grain rotation with the axis of the maximal moment of inertia³, an idea that grains *always* rotate about the axis of maximal inertia got universally accepted. The flaw with this reasoning was found in Lazarian (1994), where it was shown that thermal fluctuations within grain material induce grain wobbling, the amplitude of which depends on the ratio of the grain rotational energy E_{kin} and kT_{grain} .⁴ The quantitative theory of the effect presented in Lazarian & Roberge (1997) allowed to revise the Spitzer & McGlynn (1979) theory of crossovers (Lazarian & Draine 1997) as well as the theory of paramagnetic alignment of thermally rotating grains (Lazarian 1997a, Roberge & Lazarian 1999).

However, a more interesting development came about later, when Lazarian & Draine (1999a, henceforth LD99a) realised that grains not only wobble but occasionally flip. LD99a found that small grains flip more frequently than large ones. As the result regular torques, e.g. torques due to ejection of H_2 molecules, get averaged out over flipping grains and they get "thermally trapped", i.e. rotate at thermal velocities in spite of the presence of Purcell's torques. Taking into account that the paramagnetic alignment of thermally rotating grains is rather inefficient (see Roberge & Lazarian 1999) it is possible became possible to explain why small grain may be poorly aligned.

A new twist to the theory of grain alignment came about when Lazarian & Draine (1999b, henceforth LD99b) found that species with nuclear moments within the grain, e.g. 1H , ^{13}C , ^{27}Al , ^{31}P , ^{29}Si , $^{55}Mn...$, bring about a new type of internal relaxation which was termed "nuclear relaxation". This type of relaxation for grains larger than 10^{-5} cm happened to be $\sim 10^6$ times more efficient than the Barnett relaxation introduced in Purcell (1979). As the result, LD99b claimed that for diffuse interstellar gas nuclear relaxation thermally traps grains of the sizes from 10^{-5} – cm making the Purcell mechanism inefficient.

A group of alternative mechanisms of alignment that rely on the relative gas-grain motion have their particular niches. The first mechanical alignment mechanism was pioneered by Gold (1951). Later work included driving grains by ambipolar diffusion (Roberge & Hanany 1990, Roberge, Hanany & Messinger 1995) and Alfvén waves (Lazarian 1994, Lazarian 1997b, Lazarian & Yan 2002, Yan & Lazarian 2003). Although new efficient processes of mechanical alignment have been proposed (Lazarian 1995, Lazarian & Efrimsky 1996, Lazarian, Efrimsky & Ozik 1996), this did not make mechanical alignment universally applicable.

All this provided the background that made radiative torques mechanism most promising for explaining grain alignment over vast expanses of the interstellar space. Introduced first by Dolginov (1972) and Dolginov & Mytrophanov (1976) the radiative torques were mostly forgotten till the pioneering work by Draine & Weingartner (1996; hereafter DW96), where their efficiency was demonstrated using numerical simulations. The radiative torques make use of interaction of radiation with a grain to spin it up. Indeed, in general, one would expect that the cross sections of the interaction of an irregular grain with left and right circular polarized photons are different. As the non-polarized light can be presented as a superposition of the equal fluxes of photons with opposite circular polarization, the interaction of such a light with the irregular grain would result in grain spin up. Unlike Purcell's torques, that are fixed in grain frame, the radiative torques are expected to be less affected by grain flipping.

The predictions of radiative torque mechanism are roughly consistent with the molecular cloud extinction and emission polarimetry (Lazarian, Goodman & Myers 1997) and the polarization spectrum measured (see Hildebrand et al. 2000). They have been demonstrated to be efficient in a laboratory setup (Abbas et al. 2004). Evidence in favor of radiative torque alignment was found for the Whittet et al. (2001) data obtained at the interface of the dense and diffuse gas at the Taurus cloud (see Lazarian 2003).

In view of this success the radiative torque mechanism is the primary mechanism that we are going to study in relation to grain alignment deep inside molecular clouds. While a possible failure of radiative torques there does not exclude that grains are aligned deep within molecular clouds, their success would definitely make polarimetric studies of molecular clouds much more trustworthy and informative. Whether grains are aligned there is necessary to understand to know whether aligned grains trace only surface magnetic fields or magnetic fields deeply embedded into molecular clouds. The topology of magnetic field inside molecular clouds is essential for understanding for star formation.

It has been shown that optical and near infrared polarimetry provide magnetic fields only to A_v of 2 or less (Goodman et al. 1995, Acre et al. 1998). Is it the same for far infrared polarimetry? This is the question that we address in this paper. Earlier answers (see Lazarian et al. 1997) appeal to stars embedded in the cloud. Indeed, such stars can induce alignment through their radiation. Here we consider an extreme case of a cloud without any embedded stars. This situation is also motivated observationally, as some recent observations indicate that there are aligned grains deep in molecular clouds without high mass stars (Ward-Thompson et al. 2000).

In what follows we discuss grain alignment by radiative torque in molecular clouds. In §2, we calculate efficiency of radiative torque in a molecular cloud and minimum aligned grain sizes as a function of visual extinction in the cloud. In §3, we calculate polarized far-infrared/submillimeter emission from a pre-stellar core and discuss the relation between the degree of polarization and intensity. We give discussion in §4 and conclusion in §5.

2. RADIATIVE TORQUES

As we mentioned above, a flow of photons illuminating a grain can be presented as a superposition of left- and right-handed photons, while an irregular grain has different cross section of interaction with photons of different handedness. As the result of differential extinction, i.e. absorption and scattering, the grain feels a regular torque. Note, that the

³ Such a rotation corresponds to the minimum of grain energy for a fixed angular momentum.

⁴ It is worth noting that the amplitude of wobbling does not decrease as the efficiency of relaxation increases. The coupling between the rotational and vibrational degrees of freedom established by the relaxation mechanism acts back to induce wobbling well in accordance with Fluctuation-Dissipation Theorem (see Landau & Lifshitz 1951). More discussion of this point is given in Lazarian & Yan (2003).

key word here is regular. Random torques produced photons emitted and absorbed by a grain were discussed in terms of grain alignment by Harwit (1970). They are rather inefficient, however (Purcell & Spitzer 1971) and are more important in terms of damping of grain rotation (see Draine & Lazarian 1998).

Although the physics of grain spin up by radiative torques was for the most part properly understood by Dolginov & Mytrophanov (1976), only calculations in DW96 provided a quantitative insight into the process. These calculations obtained for test grains using Discrete Dipole Approximation code (Draine & Flatau 1994) showed that both anisotropic and isotropic radiation flows can efficiently spin-up grains. While Dolginov & Mytrophanov (1976) did understand that grains will not be only spun up, but also aligned by anisotropic radiation, they could not get correctly what would be such an alignment. Numerical simulations In Draine & Weingartner (1997) reveal complex dynamics of grains and revealed that in most cases the grains *tend* to get aligned with long axes perpendicular to magnetic field, even if paramagnetic relaxation is absent. Although the nature of this alignment in the absence of analytical calculations still remains unclear and some features of grain internal dynamics (that were discovered later!) are missing in the model studied (see an attempt in this direction in Weingartner & Draine 2003), it is very plausible that radiative torques can provide the alignment that corresponds to observations. Appealing to polarimetric data available one can claim that observations do not give us any indications that anisotropic radiation provides alignment that either has wrong sign or depends on the angle between magnetic field and anisotropy direction. This would be the case, however, if the dynamics of interstellar grains were different from the assumed one. For the rest of the paper we assume that the radiative torques do align grains with long axes perpendicular to magnetic field and will concentrate therefore only on the magnitude of radiative torques.

While calculations in DW96 were limited by the interstellar grains, we study radiative alignment of grains of larger sizes. Such grains are known to be present in molecular clouds. In addition, unlike DW96, here we are interested in the alignment of grains by attenuated and reddened interstellar light that enters into a cloud from outside.

2.1. Method

We use the DDSCAT software package (astro-ph/0309069; DW96) to calculate radiative torque on grain particles. We use the same grain shape as in DW96, which is an asymmetric assembly of 13 identical cubes. The grain is subject to radiative torque because of its irregular shape. We use the refractive index of astronomical silicate (Draine & Lee 1984; Draine 1985; Loar & Draine 1993; see also Weingartner & Draine 2001).

In our calculations, the incoming radiation is parallel to the principal axis \mathbf{a}_1 of the grain. Therefore the target orientation angle Θ , the angle between the incident radiation and the grains primary axis $\hat{\mathbf{a}}_1$ (see DW96), is zero. Therefore in our calculations the radiative torque, $\mathbf{\Gamma}_{rad}$, is parallel to $\hat{\mathbf{a}}_1$ and $|\mathbf{\Gamma}_{rad}| = |\mathbf{\Gamma}_{rad} \cdot \hat{\mathbf{a}}_1|$.

For a given wavelength and a grain size, the DDSCAT package returns the torque efficiency vector \mathbf{Q}_Γ :

$$\mathbf{Q}_\Gamma \equiv \frac{\mathbf{\Gamma}_{rad}}{\pi a_{eff}^2 u_{rad} \lambda / 2\pi}, \quad (1)$$

where $\mathbf{\Gamma}_{rad}$ is the radiative torque, $a_{eff} \equiv (3V/4\pi)^{1/3}$ the effective target radius, V the volume of the target, u_{rad} the energy density of the incident radiation, and λ the wavelength. When we consider a radiation field with the mean intensity J_λ , the radiation torque becomes

$$\mathbf{\Gamma}_{rad} = \pi a_{eff}^2 \int d\lambda (4\pi J_\lambda / c) \frac{\lambda}{2\pi} \mathbf{Q}_\Gamma, \quad (2)$$

where we used $u_{rad} = 4\pi J_\lambda / c$. When we perform the summation over λ -axis in natural logarithmic scale, the summation becomes

$$\mathbf{\Gamma}_{rad} = 2.303 \Delta(\log_{10} \lambda) (a_{eff}^2 / 2c) \sum_i (4\pi J_{\lambda,i}) \lambda_i^2 \mathbf{Q}_{\Gamma,i}, \quad (3)$$

where we used $\Delta(\log_{10} \lambda) = 2.303 d\lambda/\lambda$. Figure 1 shows that the value of $\lambda_i |\mathbf{Q}_{\Gamma,i}|$ ($= \lambda_i |\mathbf{Q}_{\Gamma,i} \cdot \hat{\mathbf{a}}_1|$) and $\lambda_i^2 |\mathbf{Q}_{\Gamma,i}|$ ($= \lambda_i^2 |\mathbf{Q}_{\Gamma,i} \cdot \hat{\mathbf{a}}_1|$) as a function of λ/a for large grains. The quantity $\lambda_i |\mathbf{Q}_{\Gamma,i}|$ is useful for integration in equation (2) and $\lambda_i^2 |\mathbf{Q}_{\Gamma,i}|$ for integration in equation (3).

Mathis, Mezger, & Panagia (1983) showed that the average interstellar radiation field (ISRF) in the solar neighborhood consists of a small UV component plus three blackbody components with $T = 3000, 4000$, and 7500 K. The blackbody components are given by

$$4\pi J_\lambda = \sum_j W(T_j) 4\pi \lambda \frac{2hc^2}{\lambda^5} \frac{1}{\exp(hc/\lambda k T_j) - 1}, \quad (4)$$

where $W(T = 3000) = 4 \times 10^{-13}$, $W(T = 4000) = 1.65 \times 10^{-13}$, $W(T = 7500) = 1 \times 10^{-14}$, $k = 1.38 \times 10^{-16}$, and $h = 6.63 \times 10^{-27}$ in cgs units. See Figure 1 of Mathis et al. (1983). Radiation field inside a giant molecular cloud located at $r_G = 5kpc$ is also given in Figure 4 of Mathis et al. (1983). They considered a spherical Giant molecular cloud that has an isotropic radiation (i.e. ISRF) incident upon the surface of the cloud. They produced the mean radiation intensity J_λ as a function of the visual extinction A_V measured from the surface of an opaque cloud. We calculate radiative torque inside a giant molecular cloud located at $r_G = 5kpc$ using the radiation field given in Mathis et al. (1983).

Once we know $\mathbf{Q}_{\Gamma,i}$ (from DDSCAT) and $J_{\lambda,i}$ (from Mathis et al. 1983), we can obtain the torque from equation (3). The gas drag damps grain angular rotation. The gas drag torque is given by

$$|\mathbf{\Gamma}_{drag,gas} \cdot \hat{\mathbf{a}}_1| = (2/3)\delta n_H(1.2)(8\pi m_H kT)^{1/2} a_{eff}^4 \omega, \quad (5)$$

where n_H is the hydrogen number density, m_H is the mass of a hydrogen atom, $\delta \approx 2$, and ω is the angular frequency (see DW96). By equating the radiative torque $|\mathbf{\Gamma}_{rad}| (= |\mathbf{\Gamma}_{rad} \cdot \hat{\mathbf{a}}_1|)$ in equation (3) and the gas drag torque $|\mathbf{\Gamma}_{drag,gas} \cdot \hat{\mathbf{a}}_1|$ above, we can obtain the angular velocity of grain rotation around $\hat{\mathbf{a}}_1$:

$$\omega_{rad} = \frac{|\mathbf{\Gamma}_{rad}|}{(2/3)\delta n_H(1.2)(8\pi m_H kT)^{1/2} a_{eff}^4} \left(\frac{1}{1 + \tau_{drag,gas}/\tau_{drag,em}} \right), \quad (6)$$

where values and definitions of the gas drag time and thermal emission drag time, $\tau_{drag,gas}$ and $\tau_{drag,em}$ respectively, are given in DW96⁵.

The thermal rotation rate ω_T is the rate at which the rotational kinetic energy of a grain is equal to $kT/2$:

$$\omega_T = \frac{15kT}{8\pi\alpha_1\rho a_{eff}^5}. \quad (7)$$

When a grain rotates much faster than ω_T , the randomization of a grain by gaseous collisions is reduced. Therefore, if a grain rotates superthermally, we expect the grain rotation axis $\hat{\mathbf{a}}_1$ is aligned with magnetic field. From equations (6) and (7), we have

$$\left(\frac{\omega_{rad}}{\omega_T} \right)^2 = \left(\frac{|\mathbf{\Gamma}_{rad}|}{(2/3)\delta n_H(1.2)(8\pi m_H kT)^{1/2} a_{eff}^4} \right)^2 \left(\frac{8\pi\alpha_1\rho a_{eff}^5}{15kT} \right)^2 \left(\frac{1}{1 + \tau_{drag,gas}/\tau_{drag,em}} \right)^2, \quad (8)$$

or,

$$\left(\frac{\omega_{rad}}{\omega_T} \right)^2 = \frac{5\alpha_1}{192\delta_2} \left(\frac{1}{n_H kT} \right)^2 \left(\frac{\rho a_{eff}}{m_H} \right)^2 \left(\gamma \int d\lambda \mathbf{Q}_{\Gamma} \lambda (4\pi J_{\lambda}/c) \right)^2 \left(\frac{1}{1 + \tau_{drag,gas}/\tau_{drag,em}} \right)^2, \quad (9)$$

where γ is the anisotropy factor of the radiation field. We use $\gamma = 0.1$ for diffuse cloud and $\gamma = 0.7$ for the GMCs in accordance with DW96. When the ratio is larger than 1, radiative torque is an efficient mechanism for grain alignment.

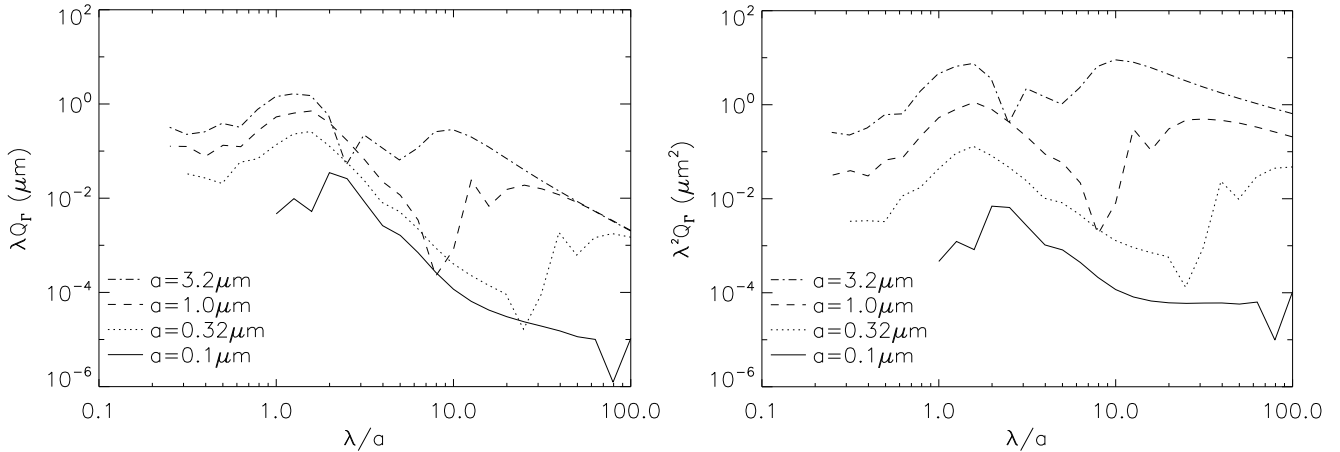


FIG. 1.— Dependence of $\lambda|\mathbf{Q}_{\Gamma} \cdot \hat{\mathbf{a}}_1|$ (left panel) and $\lambda^2|\mathbf{Q}_{\Gamma} \cdot \hat{\mathbf{a}}_1|$ (right panel) on λ/a , where λ is the wave length and a is the grain size. These quantities are useful for estimating which part of the electromagnetic spectrum contributes most to the radiative torque.

2.2. Results

We show the results for $(\omega_{rad}/\omega_T)^2$ in Figure 2. The solid line is for the interstellar radiation field (ISRF) in the solar vicinity (see Mathis et al. (1983) for details about the radiation field). DW96 used this radiation field and obtained the ω_{rad}/ω_T ratio for three grain sizes ($a_{eff} = 0.02, 0.05$, and $0.2\mu\text{m}$). In their calculation, they included both isotropic and anisotropic components of radiation field. Our calculations are slightly different. Indeed, we consider only anisotropic radiation component the effect of which on alignment is substantially stronger for the grain that we use than that of the isotropic component (see Table 4 in DW96).⁶ The calculations of radiation anisotropy in a turbulent molecular cloud made for us by Tom Bethel show that we do not overestimate γ s. On the contrary, these calculations testify that in this paper, if anything, we underestimate the actual values of radiative torques.

⁵ Additional processes, e.g. plasma drag, were discussed in Draine & Lazarian (1998). These processes are essential for small grains, but less important for large grains that we primary deal with here.

⁶ We believe that this is generally true for an ensemble of grains of arbitrary shapes, but more studies are necessary to prove this point.

Another simplification is that we consider only anisotropy of radiation only along magnetic field. This is justifiable for obtaining a crude estimate, which is the actual goal of our paper. In addition, unlike DW96, we use the UV smoothed refractive index of silicon (see Weingartner & Draine 2001). Nevertheless, our result (solid line) agrees with that of DW96 within a factor of ~ 2 .

In Figure 3, we show aligned grain size as a function of visual extinction A_V . We used Figure 2 and assumed that grains with $\omega_{rad}/\omega_T > 5$ are aligned. For a cloud with $n = 10^4$, $0.2\mu\text{m}$ grains are aligned even at $A_v \sim 4$. However, for a cloud with $n = 10^5$, $0.2\mu\text{m}$ grains are hardly aligned. Grains of $\sim 1\mu\text{m}$ are aligned even at $A_V \sim 10$ if the density does not exceed several times 10^5cm^{-3} .

In their classical paper, Mathis, Rumpl, & Nordsieck (1977; hereafter MRN), constructed a model for size distribution of dust grains in the diffuse interstellar medium (ISM). This MRN distribution has a sharp upper cutoff at $a_{max} = 0.25\mu\text{m}$. The MRN model provides a good fit to interstellar extinction and therefore widely used for modeling the diffuse ISM. It is expected that at larger optical depths the upper cutoff occurs at larger values. For example, Kim, Martin, & Hendry (1994) used the maximum entropy method and obtained a smooth decrease of size distribution starting at $0.2\mu\text{m}$. Weingartner & Draine (2001) also obtained an extended distribution beyond the MRN upper cutoff. Physically, coagulation of grains happens in denser parts of the interstellar gas (see discussion in Yan & Lazarian 2003, Yan, Lazarian & Draine 2004). Therefore it is reasonable to assume that grains larger than the usual MRN cutoff are present. Since coagulation is more frequent in dense clouds than the diffuse ISM, we expect to see a substantial amount of grains larger than $0.25\mu\text{m}$ in dense clouds (see, for example, Clayton & Mathis 1988; Vrba, Coyne, & Tapia 1993). If grains of $\sim 1\mu\text{m}$ are abundant in dark clouds, they can emit polarized infrared radiation even deep inside the cloud.

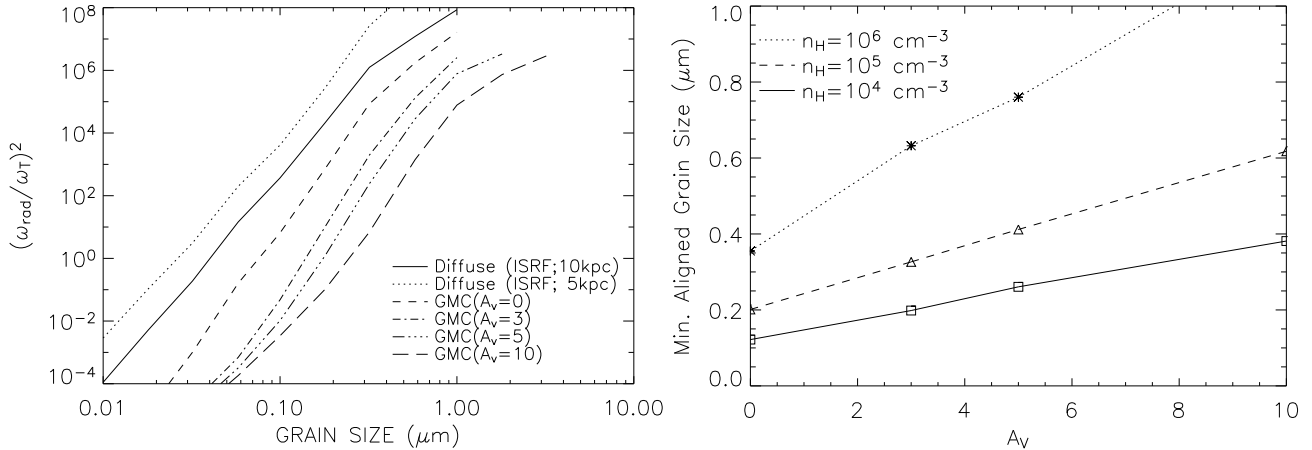


FIG. 2.— Efficiency of radiative torque. When $\omega_{rad}/\omega_T > 1$, radiative torque can rotate grains superthermally, which results in grain alignment. Different curves represent radiative torque by different radiation fields. The visual extinction A_V is for a giant molecular cloud located at 5kpc from the Galactic center. We assume $n_H = 10^4\text{cm}^{-3}$ and $T = 20\text{K}$ for the GMC (see Table 6 in DW96 for other parameters). For diffuse ISM, we use $n_H = 30\text{cm}^{-3}$ and $T = 100\text{K}$ (see Table 5 in DW96).

FIG. 3.— Minimum aligned grain size vs. visual extinction A_V . We use $T = 20\text{K}$ parameters given in DW96. However, note that we consider 3 different densities.

2.3. Polarization: Rayleigh reduction factor

In Figure 4, we plot the Rayleigh polarization reduction factor R (p. 328 in Greenberg, 1963; see also Lee & Draine 1985), which is a measure of imperfect alignment of the grain axes with respect to magnetic field. The conventional definition of the factor is $R = 1.5(\langle \cos^2 \beta \rangle - 1/3)$, where β is the angle between the grain angular momentum vector and magnetic field. The degree of polarization is reduced when some grains are not perfectly aligned in respect to magnetic field. In our case this happens for an ensemble of grains some of which, namely, small ones, are not aligned, while the other, namely, the large ones, are perfectly aligned. As the polarization for the range of far infrared λ and grain sizes a does not depend on those parameters, we can calculate the reduction factor for the entire distribution of grains as follows:

$$R = \frac{\int_{a_{aligned}}^{a_{max}} C_{ran} n(a) da}{\int_{a_{min}}^{a_{max}} C_{ran} n(a) da}, \quad (10)$$

where C_{ran} is the cross-section, $n(a)$ the grain number density, a the grain size, a_{min} the minimum size of grains, a_{max} the maximum size, and $a_{aligned}$ the minimum aligned size, which is given in Figure 3. We assume MRN-type power-law grain size distributions:

$$n(a) \propto a^{-3.5} \quad (11)$$

for $a = 0.005\mu\text{m}$ to $a = a_{max} \mu\text{m}$. We consider two values for a_{max} : the original MRN cutoff at $a_{max} = 0.25\mu\text{m}$ and a larger cutoff at $a_{max} = 1\mu\text{m}$ for the calculation of R . We show the results in Figure 4(a) and 4(b), respectively.

For the original MRN distribution (Figure 4(a)), R is smaller than ~ 0.4 for $n_H > 10^4 \text{ cm}^{-3}$. However, for the larger upper cutoff (Figure 4(b)), R is about ~ 0.2 inside clouds at $A_V = 10$ when $n_H \sim 10^5 \text{ cm}^{-3}$.

We present the results for an opaque giant molecular cloud located at 5kpc from the Galactic center. As we explained earlier, we used radiation field given in Mathis et al. (1983). They calculated the radiation field assuming that the visual extinction A_V at the center measured from the surface is 200. However, as long as the central visual extinction is larger than ~ 15 , the radiation field may not be sensitive to the choice of the central A_V (see Flannery, Roberge, & Rybicki, 1980). Therefore, our qualitative results obtained here are applicable to various astrophysical objects - from dense prestellar cores to giant molecular clouds.

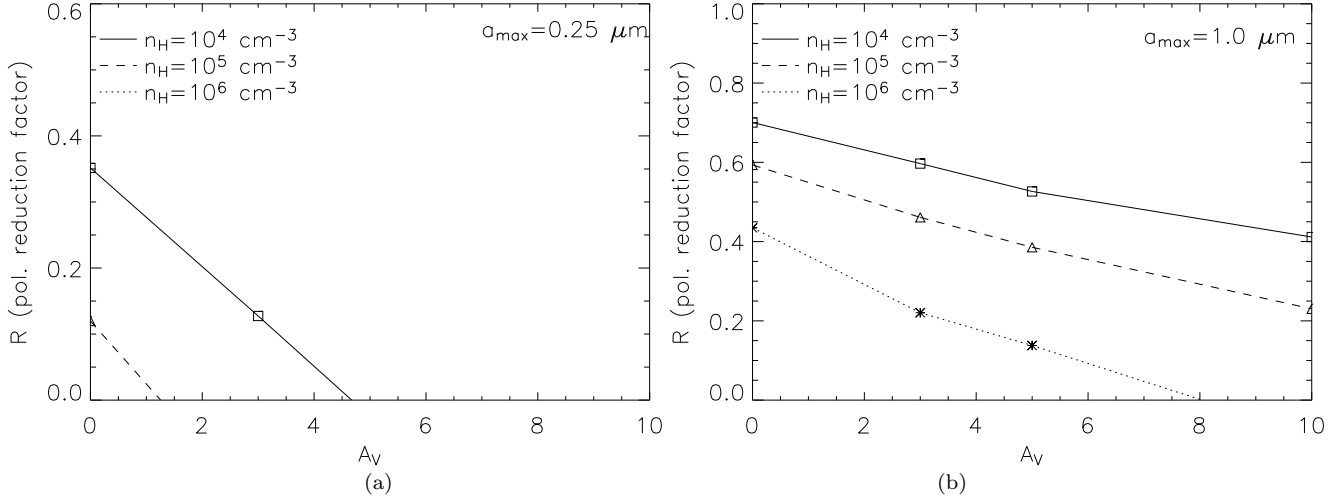


FIG. 4.— Rayleigh polarization reduction factor (see equation (10) for the definition in our case). (a) The original MRN distribution with $a_{max} = 0.25 \mu\text{m}$. (b) An extended MRN distribution with $a_{max} = 1.0 \mu\text{m}$.

3. POLARIZED EMISSION FROM A DARK CORE

In the previous section, we showed that larger grains can rotate super-thermally even at $A_V = 10$ in giant molecular clouds. In this section, we apply the result to dense pre-stellar cores. As we noted at the end of the last section, we obtained the results in the previous section using the radiation field suitable for giant molecular clouds. Therefore, it is questionable whether or not we can directly apply the results in the previous section to prestellar cores. However, judging from Flannery et al. (1980) calculation, we expect that the direct application is ill-justified only near the very center of the cores.

3.1. Method

In this section we calculate polarized emission from a dark pre-stellar core. We assume a simple spherically symmetric density distribution and a constant temperature ($T \sim 20\text{K}$). We take density profile of logatropic sphere (Lizano & Shu 1989; McLaughlin & Pudritz 1996), which has a finite central density and a $\rho \propto r^{-1}$ envelope. The logatropic sphere is supported by turbulent pressure (and isothermal gas pressure in its original form). The turbulent pressure represents nonthermal velocity dispersion observed in clouds. The density profile of a logatropic sphere is different from the critically stable isothermal Bonner-Ebert sphere (Bonner 1956; Ebert 1955), which has a $\rho \propto r^{-2}$ envelope. Although some observations (e.g. Alves et al. 1998; Lada, Alves, & Lada 1999; Johnstone & Bally 1999) support the $\rho \propto r^{-2}$ profile, other observations (e.g. van der Tak et al. 2000; Colome, di Francesco, & Harvey 1996; Henning et al. 1998) support the other profile. For simplicity, we use

$$\rho(r) \propto \begin{cases} \text{constant} & \text{if } r < r_0/4.7 \\ r^{-1} & \text{otherwise,} \end{cases} \quad (12)$$

where r_0 is a parameter in our calculations (see McLaughlin & Pudritz 1996 for its physical meaning) and we set the central number density $n_{H,c}$ to $3 \times 10^5 \text{ cm}^{-3}$. This distribution truncates at $r \sim 24r_0$. We take a magnetic field from our earlier direct 3-dimensional numerical simulation (see Cho & Lazarian 2003). Numerical resolution is 216^3 and the average Mach number is ~ 7 . The magnetic field has both uniform and random components. The strength of the mean field is about 2 times stronger than the fluctuating magnetic field. We assume that the uniform field is perpendicular to the line of sight of the observer.

We assume that the visual extinction A_V at the center measured from the surface is ~ 10 . This means that the total column density through the center is about $N_H \sim 3.7 \times 10^{22} \text{ cm}^{-2}$. The size of the cloud corresponds to $\sim 0.02 \text{ pc}$. This cloud is similar to, for example, L183 (see Crutcher et al. 2004).

We assume an MRN type grain size distribution, $n(a) \propto a^{-3.5}$, from $a = 0.005 \mu\text{m}$ to $a = a_{max}$. Unlike the original MRN distribution, where $a_{max} = 0.25 \mu\text{m}$, we use a_{max} of up to $2 \mu\text{m}$. We assume that grains are oblate spheroid with the axial ratio of ~ 1.2 , which is smaller than the value used by Padoan et al. (2001).

We follow the method somewhat modified from the one in Fiege & Pudritz (2000) to compute the polarization maps. Here we briefly describe the procedures. It is natural to assume (see Fiege & Pudritz 2000) that one can ignore the effects of absorption and scattering when dealing with submillimeter wavelengths. Therefore the polarization submm range is due to pure emission. The Stokes parameters are given by

$$Q \propto C_{pol} R q, \quad (13)$$

$$U \propto C_{pol} R u, \quad (14)$$

$$I \propto C_{ran} \left[\int \rho ds - \frac{C_{pol} R}{C_{ran}} \int \rho \left(\frac{\cos^2 \gamma}{2} - \frac{1}{3} \right) ds \right], \quad (15)$$

where

$$C_{pol} = C_{\perp} - C_{\parallel}, \quad (16)$$

$$C_{ran} = (2C_{\perp} + C_{\parallel})/3, \quad (17)$$

$$q = \int \rho \cos^2 \psi \cos^2 \gamma ds, \quad (18)$$

$$u = \int \rho \sin^2 \psi \cos^2 \gamma ds, \quad (19)$$

R is the polarization reduction factor, ψ the angle between the projection of the local \mathbf{B} on the plane of the sky and north, and γ is the angle between the local \mathbf{B} and the plane of the sky. As explained earlier, the factor R is the n reduction factor due to imperfect grain alignment. Note that $a_{aligned}$ is a function of both n_H and A_V . Figure 3 shows how $a_{aligned}$ is related to n_H and A_V . Based on the figure we assume that

$$a_{aligned} = [\log_{10}(n_H)]^3 (A_V + 5)/2800 \mu\text{m}. \quad (20)$$

The error of this fitting formula is around $\sim 10\%$. Note that this fitting formula does not have any physical background. From Q , U , and I , we can obtain polarization angle χ and the degree of polarization as follows:

$$\tan 2\chi = u/q, \quad (21)$$

$$P = \frac{\sqrt{Q^2 + U^2}}{I}. \quad (22)$$

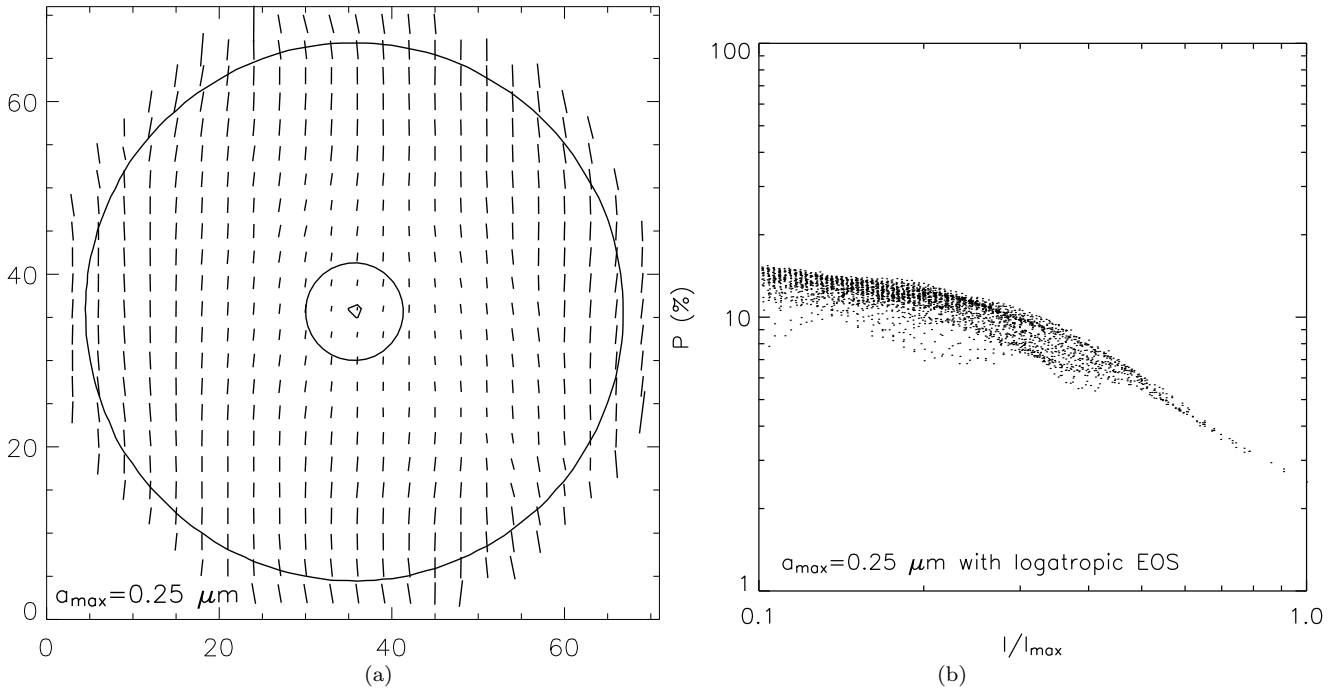


FIG. 5.— Polarization map and p-I scatter diagram for the original MRN distribution (i.e. $a_{max} = 0.25$). We use a logatropic sphere for density, which has a $\rho \propto r^{-1}$ envelop. (a) From the center to the boundary, contours represent 90%, 50%, and 10% of the maximum intensity. (b) The scatter diagram follows $p \propto I^1$ near the center.

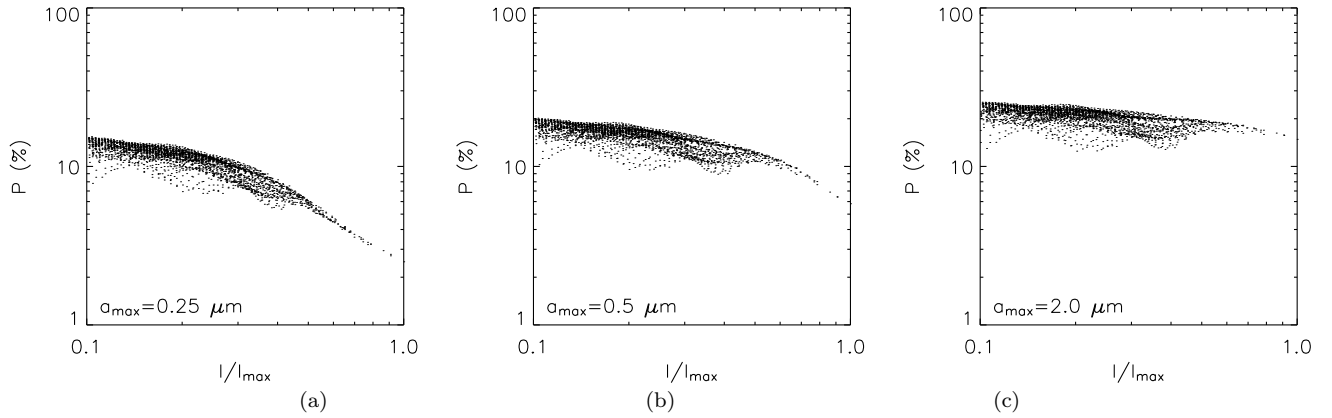


FIG. 6.— The slope gets flatter as the upper cutoff, a_{max} , increases. This is because larger cutoff means more aligned grains near the cloud center and, therefore, higher polarization intensity. (a) $a_{max} = 0.25\mu\text{m}$. (b) $a_{max} = 0.5\mu\text{m}$. (c) $a_{max} = 2.0\mu\text{m}$.

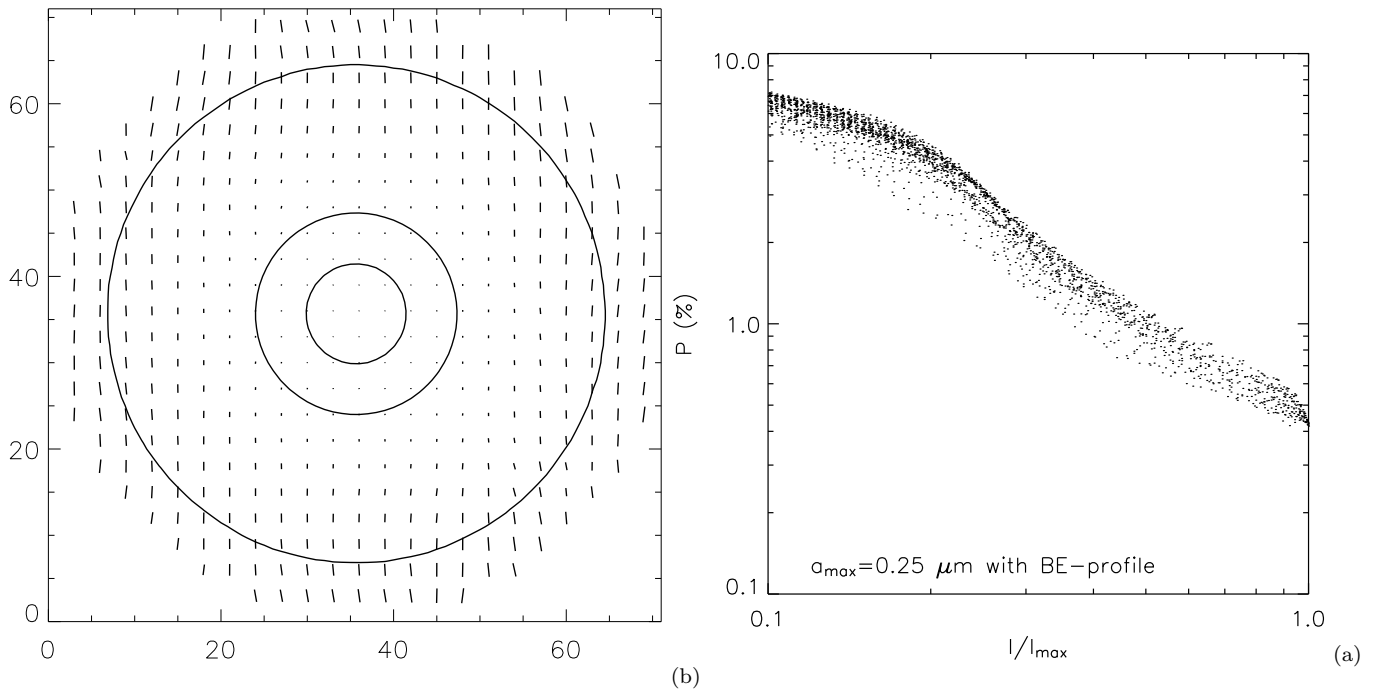


FIG. 7.— Polarization map and p-I scatter diagram for the original MRN distribution (i.e. $a_{max} = 0.25$). We use the isothermal Bonner-Ebert sphere for density, which has a $\rho \propto r^{-2}$ envelop. (a) Polarization map. Contours represent 90%, 50%, and 10% of the maximum intensity. (b) p-I relation.

3.2. Simulated map and p-I relation

In Fig. 5(a), we plot the polarization map for the original MRN distribution with $a_{max} = 0.25\mu\text{m}$. We clearly observe the depolarization effect, namely, the degree of polarization decreases toward the cloud center. On the other hand, the intensity of dust IR emission is strongest at the center. Three contours represent 90%, 50%, and 10% of the maximum intensity. In Figure 5(b), we plot the degree of polarization (p) vs. intensity (I).

Many observations show that the degree of polarization (p) decreases as intensity (I) increases. The relation is usually fitted by a power law. However, the exact power law index varies. Matthews & Wilson (2000) reported $p \propto I^{-0.7}$ for the OMC-3 region of the Orion A. On the other hand, Matthews & Wilson (2002) obtained $p \propto I^{-0.8}$ for the dense cores in Barnard 1. For other dense cores, Henning et al. (2001) reported $p \propto I^{-0.6}$, Lai et al. (2002) $p \propto I^{-0.8}$, and Crutcher et al. (2004) $p \propto I^{-1.2}$. See Figure 1 of Goncalves, Galli, & Walmsley (2004) for illustration.

We claim that the power law index is sensitive to the value of a_{max} . In Figure 6, we show the change of slopes as a function of the upper cutoff a_{max} . The flattening of the slope can be understood as follows. When a_{max} gets larger, large grains become relatively more abundant. Since larger grains are aligned even near the cloud center, we expect higher degree of polarization near the center. Therefore, the depolarization effect becomes less pronounced and the slope gets flatter. We leave for further studies to establish whether or not the actual slope of the curve can be used to

constrain the grain size distribution.

For the sake of completeness, we also calculate the polarization map and p-I diagram for the isothermal Bonner-Ebert sphere. We take the same central density and other parameters as in the logatropic sphere. In Figure 7(a), we observe more pronounced depolarization effect, which is because of steeper density gradient. The p-I scatter diagram in Figure 7(b) reflects this.

4. DISCUSSION

Our calculations show a substantial increase of radiative torque efficiency as the grain size grows. For the power-law distribution of grain sizes we have shown that the p-I relation is sensitive to a_{max} and the density profile of clouds. Power-law distribution as an approximation for an actual grain size distribution was used only for illustrative purpose. For instance, in Weingartner & Draine (2001) the grain distribution is approximated by a power law up to a_{max} and an exponential tail of grains larger than a_{max} . It is clear from our calculations that if grains with the size of a_{max} are aligned, the grains within the exponential tail should also be aligned. In fact, the answer to a very important question whether far infrared polarization reflects the structure of magnetic field at high optical depths does not depend on the details of the assumed distribution of grains. It is only essential that a substantial percentage of dust mass be in sufficiently large grains. If we want to predict a polarization spectrum (see Hildebrand et al. 2000) then the size distribution of grains would matter. For instance, grains of different sizes can have different temperatures and contribute to either polarized or not polarized parts of radiation. For clouds with embedded stars, the polarization spectrum would depend on the distribution of stars as well.

In practical terms our major result is that large grains must be aligned even at high optical depths. This makes sub-millimeter polarimetry (see Novak et al. 2003) a useful tool for studies of magnetic fields through the entire process of star formation. An earlier understanding reflected in, for instance, Lazarian, Goodman & Myers (1997) was that embedded stars are essential for revealing structure of magnetic fields at large optical depth. This meant that polarimetry might not be able to reveal the role of magnetic fields at the initial stages of star formation. It is worth mentioning, that observational evidence that grains are aligned in the conditions when the radiation field is substantially reduced have been recently claimed to be a major challenge to grain alignment theory (see Goncalves, Galli & Walmsley 2005).

How can we explain that the optical and near infrared polarimetry does not detect an appreciable polarization signal originating at high optical depth? We believe that this stems from the fact that the optical and near infrared extinction is biased towards small grains which are not aligned. Qualitatively the nature of the bias can be understood if one recalls that for $\lambda < 2\pi a_c$ the efficiency of the grains in producing polarized signal drops. At the same time the grains with $a > a_c$ continue to extinct light. Therefore if a substantial number of grains are larger than a_c the dichroic properties of the medium in terms of the transmitted light are affected only by grains from $a_{aligned}$ given by eq.(20) to $\sim a_c$. At the same time for grain emission at $\lambda \gg 2\pi a$ the degree of polarization is determined by the grains from $a_{aligned}$ to a_{max} .

To illustrate the situation when both near infrared and far infrared polarimetry would show similar results consider a case of the grain alignment at the interface of the diffuse-dense cloud described in Whittet et al. (2001). For the range of near-infrared measurements from $0.35 \mu\text{m}$ to $2.2 \mu\text{m}$ the optical cross section of grains less than $0.25 \mu\text{m}$ is still proportional to a^3 . For the case of the Taurus Dark Clouds Whittet et al. (2001) showed that for low optical extinctions, i.e. $0 < A_v < 3$ the ratio of the total to selective extinction stays similar to the value of it in the diffuse gas, i.e. $R_v \approx 3$, while the wavelength of maximal polarization λ_{max} that enters Serkowski law (i.e. $p_\lambda/p_{max} = \exp[-K \ln^2(\lambda_{max}/\lambda)]$), increases. Whittet et al. (2001) interpreted this as the result of the size-dependent variations in grain alignment. Lazarian (2003) explained this as the consequence of the radiative torques which fail to align small grains at higher optical depths. Our results here support this conclusion. Indeed, if we adopt the grain-size distribution with the original cut-off corresponding to the diffuse medium, i.e. $a_{max} = 0.25 \mu\text{m}$, using our Figure 3 and eq.(10) we get Rayleigh reduction factor (or effective alignment) around ten percent at $A_v = 3$, which is a substantial reduction from the value ≈ 1 for A_v of 1.

At high optical depth the grain-size distributions are rather uncertain. To illustrate the importance of grain size growth⁷ for alignment, let us use the distribution in WD01 corresponding to $R_v = 5.5$ for A_v of 10 and $n_H = 10^4 \text{ cm}^{-3}$. According to Fig. 3 only grains with $a > 0.6 \mu\text{m}$ are aligned. According to WD01 the favored distribution of silicate grains is cut-off at a smaller grain size. Therefore they are not aligned. The carbonaceous grains have a distribution with a cut-off at $\sim 1 \mu\text{m}$. As the result we expect $R^{carb} \sim 0.4$, which is larger than the value of effective alignment for A_v of 3 in the previous example⁸. If we use another model of WD01 corresponding to $R_v = 5.5$ that has MRN-type distribution of carbonaceous grains up to size $a \sim 10 \mu\text{m}$, then the R^{carb} gets close to 0.8! With all these uncertainties we clearly see that far-infrared polarimetry can get insight into the magnetic field topology at large optical depths. In fact, we believe that far-infrared polarimetry allows consistency checks for the models of grain-size distributions.

All these results are valid for clouds without embedded massive stars. The radiation field is being enhanced in the clouds and therefore we expect more aligned grains. If grain size distribution stays the same as in dark clouds, we expect to have high degrees of far-infrared polarization but still relatively little polarization in terms of optical

⁷ It is important to realize that the increase of the upper cutoff for the grain size happens partially due to coagulation of smaller grains. Therefore this could be achieved without mantle growth. Naturally, the models with larger grains, i.e. WD01 do not violate the dust-to-gas ratio.

⁸ We expect to have polarization of the level of ≈ 3 percent for this case in emission.

and near-infrared polarimetry. The details of this picture can be tested using polarization spectrum technique in Hildebrand et al (2000).

We would claim that establishing why some grains are not aligned are as important as determining why other grains are aligned. These are two inseparable parts of the grain alignment problem that must be solved to make aligned grains a reliable technique for magnetic field study. On the basis of the present work we believe that we can account for the polarization arising from dust in dark clouds. Thermal flipping in the presence of the nuclear spin relaxation described in Lazarian & Draine (1999b) accounts why small grains are not aligned by Purcell's torques. Therefore we believe that we have a qualitative agreement between the theory and observations (cf. Goncalves et al. 2004). We provide a qualitative comparison of the theory and observations in another paper, where we do radiative transfer in a model of a fractal molecular cloud.

Can the alignment be higher than we predict? Yes, we dealt only with radiative torques. In fact, calculations in Lazarian & Draine (1999b) show that for sufficiently large grains thermal flipping is not important. As the result such grains are not thermally trapped and can rotate fast in accordance with Purcell's original predictions. Naturally, these grains will be aligned paramagnetically. The requirement for Purcell's torques to work in dark clouds is for a residual concentration (a fraction of a percent) of atomic hydrogen to be present or for the grains to have temperatures different from gas. In addition, MHD turbulence can move grains mostly perpendicular to magnetic field lines and align them (Yan & Lazarian 2003). All these mechanisms are likely to act in unison increasing the alignment of grains with longer axes perpendicular to magnetic field lines.

Our calculations have been motivated by grain alignment in molecular clouds. Large grains are known to be present in accretion disks around stars, e.g. protoplanetary disks. Our work is suggestive that such grains should be aligned and therefore reflect the structure of magnetic field in disks. As magnetic fields are believed to play an important role in accretion, the importance of this is difficult to overestimate.

The limitation of our calculation is that we used a magnetic field from a homogeneous MHD simulation without self-gravity. In reality, the magnetic field near dense clouds can be very different from the one we used here. Recent calculation by Goncalves et al. (2004) shows that hour glass type magnetic field combined with a torus-like density profile can cause a depolarized emission from the cloud center. The reduction factor is around 2. Therefore, we expect further reduction of polarization when we use a more realistic magnetic field.

It is also worth mentioning that the radiation fields given in Mathis et al. (1983) is based on the assumption that the cloud is spherical and uniform. Real molecular clouds are likely to be inhomogeneous and, possibly, hierarchically clumpy. As a result, the radiation has more chances to penetrate deep within molecular clouds (see Mathis, Whitney, & Wood, 2002) to allow grains to be aligned at much higher A_V . Elsewhere we have obtain the radiation field inside inhomogeneous clouds using direct numerical technique similar to the one in Bethell et al. (2004) and intend to improve our present work by combining our results here and a more realistic cloud model with realistic radiation field.

The ability to trace magnetic fields inside molecular clouds is difficult to overestimate. Using Chandrasekhar & Fermi (1953) technique one can infer magnetic fields strength both in the cloud and cloud envelope to test whether star formation takes place in sub or supercritical regimes (see Crutcher 2004). The magnetic connection between clouds and cloud cores is also essential for understanding the processes star formation. Does magnetic reconnection plays important role for removing the magnetic flux from molecular clouds? This can be answered by studies of magnetic field topology. In fact, the study of magnetic topology inside molecular clouds could test different models of magnetic reconnection, e.g. those discussed in Shay et al. (1998) and Lazarian, Vishniac & Cho (2004). In addition, polarimetry studies of magnetic field structure can bring important insight into the structure of MHD turbulence insight molecular clouds (see review by Lazarian & Yan 2005 and references therein).

Our finding confirm that the present day understanding of grain alignment can account for all the observational data currently available. This makes us believe that polarization arising from aligned grains has become a tool based on solid theoretical foundations. The latter is important not only for molecular cloud studies but for many other studies, e.g. those of comet, circumstellar polarimetry (see Lazarian 2003 and references therein) as well as for predicting and interpolating to other wavelength the polarized foreground contribution from dust (see review by Lazarian & Finkbeiner 2004 and references therein).

5. SUMMARY

We have studied the efficiency of grain alignment by radiative torque in optically thick clouds. We have established that the efficiency of radiative torques is a steep function of the grain size. As the result, even deep inside giant molecular clouds ($A_V \lesssim 10$), large grains can be aligned by radiative torque. This means that far-infrared/submillimeter polarimetry can reliably reflect the structure of magnetic field deep inside molecular clouds. Our results show that the grain size is important for determining the relation between the degree of polarization and intensity from molecular cloud dust.

This work is supported by NSF grant AST-0243156 and the NSF Center for Magnetic Self-Organization in Laboratory and Astrophysical Plasmas. This work utilized CITA supercomputing facilities during its early stages. We thank Bruce Draine, Dick Crutcher, Roger Hildebrand, John Mathis, and Giles Novak for useful discussions.

REFERENCES

- | | |
|--|--|
| Abbas, M., Craven, P., Spann, J., Tankosic, D., LeClair, A.,
Gallagher, D., West, E., Weingartner, J., Witherow, W., &
Tielens, A. 2004, ApJ, 614, 781 | Alves, J., Lada, C., Lada, E., Kenyon, S., & Phelps, R. 1998, ApJ,
506, 292 |
|--|--|

- Arce, H., Goodman, A., Bastien, P., Manset, N., Sumner, M. 1998, 499, 93
- Bethell, T., Zweibel, E., Heitsch, F., & Mathis, J. 2004, ApJ, 610, 801
- Bonner, W. 1956, MNRAS, 116, 351
- Chandrasekhar, S. & Fermi, E. 1953, ApJ, 118, 113
- Cho, J. & Lazarian, A. 2003, MNRAS, 345, 325
- Clayton, C., & Mathis, J. 1988, ApJ, 327, 911
- Colome, C., di Francesco, J., & Harvey, P. 1996, ApJ, 461, 909
- Crutcher, R. 2004, in Magnetized Interstellar Medium, eds. B.Uyaniker, W. Reich, and R. Wielebinski, Copernicus, Katlenburg-Lindau, p. 123
- Crutcher, R., Nutter, D., Ward-Thompson, D., & Kirk, J. 2004, ApJ, 600, 279
- Davis, L. & Greenstein, J.L. 1951, ApJ, 114, 206
- Dolginov A.Z. 1972, Ap&SS, 16, 337
- Dolginov A.Z. & Mytrophanov, I.G. 1976, Ap&SS, 43, 291
- Draine, B. & Flatau, P. 1994, J. Opt. Soc. Am. A., 11, 1491
- Draine, B. & Lee, H. 1984, ApJ, 285, 89
- Draine, B. 1985, ApJS, 57, 587
- Draine, B., Lazarian, A. 1998, ApJ, 508, 157
- Draine, B. & Weingartner, J. 1996, ApJ, 470, 551 (DW96)
- Draine, B. & Weingartner, J. 1997, ApJ, 480, 633
- Ebert, R. 1955, Z. Astrophys., 37, 217
- Fiege, J. & Pudritz, R. 2000, ApJ, 544, 830
- Flannery, B., Roberge, W., & Rybicki, G. 1980, 236, 598
- Goncalves, J., Galli, D., & Walmsley, M. 2005, A&A, 430, 979
- Goodman, A., Jones, T., Lada, E., & Myers, P. 1995, ApJ, 448, 748
- Gold, T. 1951, Nature, 169, 322
- Greenberg, M. 1968, in *Stars and Stellar Systems*, Vol. 7, *Nebulae and Interstellar Matter*, ed. B. Middlehurst and L. Aller (Chicago: University of Chicago Press), p. 221
- Hall, J. 1949, Science, 109, 166
- Henning, T., Burket, A., Launhardt, R., Leinert, C., & Stecklum, B. 1998, A&A, 336, 565
- Henning, T., Wolf, S., Lannhardt, R., & Waters, R. 2001, ApJ, 561, 871
- Hildebrand, R., Davidson, J. A., Dotson, J.L., Wovell, C.D., Novak, G., & Vaillancourt, J.E. 2000, PASP, 112, 1215
- Hildebrand, R. 2002, in *Astrophysical Spectropolarimetry*, ed. by J. Trujillo-Bueno, F. Moreno-Insertis, & F. Sanchez (Cambridge, UK: Cambridge Univ. Press), p. 265
- Hiltner, W. 1949, Science, 109, 165
- Johnston, D., & Bally, J. 1999, ApJ, 510, L49
- Kim, S.-H. & Martin, P. 1995, ApJ, 444, 293
- Kim, S.-H., Martin, P., & Hendry, P. 1994, ApJ, 422, 164
- Lada, C., Alves, J., & Lada, E. 1999, ApJ, 512, 250
- Lai, S.-P., Girart, J., & Crutcher, R. 2003, ApJ, 598, 392
- Landau, L. & Lifshitz, E. 1976, Statistical Physics, part 1, second edition, Nauka, Moscow
- Lazarian, A. 1994, MNRAS, 268, 713
- Lazarian, A. 1995, ApJ, 453, 229
- Lazarian, A. 1997a, MNRAS, 288, 609
- Lazarian, A. 1997b, ApJ, 483, 296
- Lazarian, A. 2003, Journal of Quantitative Spectroscopy and Radiative Transfer, 79, 881
- Lazarian, A. & Draine, B. 1999a, ApJ, 516, L37
- Lazarian, A. & Draine, B. 1999b, ApJ, 520, L67
- Lazarian, A., Efrimsky, M., & Ozik, J. 1996, ApJ, 472, 240
- Lazarian, A. & Efrimsky, M. 1996, ApJ, 466, 274
- Lazarian, A., Goodman, A.A., & Myers, P.C. 1997, ApJ, 490, 273
- Lazarian, A. & Roberge, W. 1997, ApJ, 484, 230
- Lazarian, A., Vishniac, E., & Cho, J. 2004, 603, 180
- Lazarian, A., & Yan, H. 2002, ApJ, 566, L105
- Lazarian, A., & Yan, H. 2003, in Astrophysics of Dust, eds. Adolf N. Witt, Geoffrey C. Clayton, and Bruce T. Draine, ASP, 309, 479
- Lazarian, A., & Yan, H. 2005, preprint, astro-ph
- Laor, A. & Draine, B. 1993, ApJ, 402, 441
- Lee, H. & Draine, B. 1985, ApJ, 290, 211
- Lizano, S. & Shu, F. 1989, ApJ, 342, 834
- Matthews, B. & Wilson, C. 2000, ApJ, 531, 868
- Matthews, B. & Wilson, C. 2002, ApJ, 574, 822
- Mathis, J., Whitney, B., & Wood, K. 2002, ApJ, 574, 812
- Mathis, J., Mezger, P., & Panagia, N. 1983, A&A, 128, 212
- Mathis, J., Rimpl, W., & Nordsieck, K. 1977, ApJ, 217, 425 (MRN)
- McLaughlin, D. & Pudritz, R. 1996, ApJ 469, 194
- Novak, G., Chuss, D.T., Renbarger, T., Griffin G.S., Newcomb, M.G., Peterson, J.B., Loewenstein, R.F., Pernic, D., Dotson, J.L. 2003, ApJ, 583, 83
- Padoan, P., Goodman, A., Draine, B., Juvela, M., Nordlund, ØA., & Rögnvaldsson, O. 2001, ApJ, 559, 1005
- Padoan, P. & Norlund, ØA. 1999, ApJ, 526, 279
- Purcell, E. 1969, Physica, 41, 100
- Purcell, E. 1975, in Dusty Universe, eds. Field G.B., Cameron, A.G.W., New York: Neal Watson, 155
- Purcell, E. 1979, ApJ, 231, 404
- Purcell, E. & Spitzer, L. 1971, ApJ, 167, 31
- Roberge, W. & Hanany, S. 1990, B.A.A.S., 22, 862
- Roberge, W., Hanany, S., & Messinger, D. 1995, 453, 238
- Roberge, W.G., & Lazarian, A. 1999, MNRAS, 305, 615
- Shay, M., Drake, J., Denton, R., & Biskamp, D. 1998, J. Geophys. Res., 103, 9165
- Spitzer, L. & McGlynn, T. 1979, ApJ, 231, 417
- Spitzer, L. & Tukey, 1951, ApJ, 114, 187
- van der Tak, F., van Dishoeck, E., Evans, N., & Blake, G. 2000, ApJ, 537, 283
- Vrba, F., Coyne, G., & Tapia, S. 1993, AJ, 105, 1010
- Ward-Thompson, D., Kirk, J.M., Crutcher, R.M., Greaves, J.S., Holland, W.S., & Andre, P. 2000, ApJ, 537, L135
- Ward-Thompson, D., Andre, P., & Kirk, J. 2002, MNRAS, 329, 257
- Weingartner, J. & Draine, B. 2001, ApJ, 548, 296
- Weingartner, J. & Draine, B. 2003, ApJ, 589, 289
- Whittet, D.C.B., Gerakines, P.A., J.H. Hough, & Shenoy 2001, ApJ, 547, 872
- Yan, H. & Lazarian, A. 2003, ApJ, 592, 33
- Yan, H., Lazarian, A., & Draine, B. 2004, ApJ, 616, 895